THE JOURNAL OF COMPARATIVE NEUROLOGY 505:669–681 (2007)

Auditory Brainstem Neural Activation Patterns Are Altered in EphA4- and Ephrin-B2-Deficient Mice

ILONA J. MIKO,[1] PAUL A. NAKAMURA,[1] MARK HENKEMEYER,[2] AND KARINA S. CRAMER[1]*

[1]Department of Neurobiology and Behavior, University of California Irvine, Irvine, California 92697

[2]Department of Developmental Biology, UT Southwestern Medical Center, Dallas, Texas 75390

ABSTRACT

Auditory processing requires proper formation of tonotopically ordered projections. We have evaluated the role of an Eph receptor tyrosine kinase and an ephrin ligand in the development of these frequency maps. We demonstrated expression of EphA4 and ephrin-B2 in auditory nuclei and found expression gradients along the frequency axis in neonates. We tested the roles of EphA4 and ephrin-B2 in development of auditory projections by evaluating whether mutations result in altered patterns of expression of the immediate early gene *c-fos* after exposure to pure tone stimuli. We evaluated two nuclei, the dorsal cochlear nucleus (DCN) and the medial nucleus of the trapezoid body (MNTB), which project in two distinct auditory pathways. The mean number of c-fos-positive neurons in *EphA4*$^{-/-}$ DCN after 8-kHz pure tone stimulation was 42% lower than in wild-type DCN. Along the dorsoventral, tonotopic axis of DCN, the mean position of c-fos-positive neurons was similar for mutant and wild-type mice, but the spread of these neurons along the tonotopic axis was 35% greater for *ephrin-B2*$^{lacZ/+}$ mice than for wild-type mice. We also examined these parameters in MNTB after exposure to 40-kHz pure tones. Both *EphA4*$^{-/-}$ and *ephrin-B2*$^{lacZ/+}$ mice had significantly fewer c-fos-positive cells than wild-type littermates. The labeled band of cells was narrower and laterally shifted in *EphA4*$^{-/-}$ mice compared with wild-type mice. These differences in cell number and distribution suggest that EphA4 and ephrin-B2 signaling influence auditory activation patterns. J. Comp. Neurol. 505: 669–681, 2007.

Indexing terms: auditory; brainstem; ephrin; Eph receptor; development; topography; tonotopy; c-fos

Central auditory projections in the brainstem are topographically organized, reflecting the highly ordered arrangement of best frequencies originating in the cochlea (Friauf and Lohmann, 1999; Rubel and Fritzsch, 2002). This tonotopy is observed at early postnatal ages in mammals (Snyder and Leake, 1997; Leake et al., 2002). Tonotopy is subsequently refined to some degree in several pathways in the auditory brainstem, including the cochlear nucleus (Leake et al., 2002) and the superior olivary complex (Sanes and Constantine-Paton, 1985; Kim and Kandler, 2003); however, these studies show a significant degree of tonotopy prior to refinement. The establishment of tonotopic projections thus relies on activity-independent mechanisms and on activity-dependent refinement, both of which participate in the formation of maps (Pfeiffenberger et al., 2006).

Activity-independent mechanisms include signaling through axon guidance molecules. The Eph family proteins, consisting of Eph receptors and their ligands, the ephrins, form a large family of axon guidance molecules. Eph proteins contain the A and B classes. Generally, ephrin-A ligands bind to EphA receptors, and ephrin-B

Grant sponsor: National Institutes of Health; Grant number: DC005771; Grant number: DC006225; Grant number: T32 NS045540.

*Correspondence to: Dr. Karina S. Cramer, 2205 McGaugh Hall, Department of Neurobiology, University of California, Irvine, Irvine, CA 92697. E-mail: cramerk@uci.edu

Received 22 March 2007; Revised 24 May 2007; Accepted 11 September 2007

DOI 10.1002/cne.21530

Published online in Wiley InterScience (www.interscience.wiley.com).

ligands bind to EphB receptors; in addition, ephrin-B2 binds to EphA4 and ephrin-A5 binds to EphB2 (Gale et al., 1996; Himanen et al., 2004). Interactions between Eph receptors and ephrins mediate cell–cell contacts in a repulsive manner but can be attractive as well (Flanagan and Vanderhaeghen, 1998; Wilkinson, 2001; McLaughlin et al., 2003; Hansen et al., 2004). Eph proteins have an important role in the formation of topography in several regions of the nervous system, most notably in the early visual pathways in which deletion of these proteins alters the anatomical maps (Frisen et al., 1998; Feldheim et al., 2000, 2004). Relative levels of expression within gradients facilitate the formation of topographic maps (Reber et al., 2004; McLaughlin and O'Leary, 2005). Mutant mice lacking ephrins show functional changes in cortical maps in response to visual (Cang et al., 2005) as well as somatosensory (Prakash et al., 2000) stimulation. Eph protein signaling, in addition to guiding axon outgrowth, also regulates the maturation of synapses (Dalva et al., 2007).

The demonstration that Eph protein interactions contribute to the formation of topographic maps suggests that they are candidate molecules for initiating tonotopic maps in the auditory brainstem. Previous studies have shown that Eph family proteins are expressed in peripheral and auditory pathways in chick (Cramer et al., 2000, 2002; Bianchi and Gray, 2002; Person et al., 2004; Siddiqui and Cramer, 2005) and mice (Henkemeyer et al., 1994; Ellis et al., 1995; Rogers et al., 1999; Pickles et al., 2002). Moreover, functional studies have shown that Eph signaling influences axon outgrowth and guidance in the chick brainstem (Cramer et al., 2004, 2006). One family member, EphA4, is expressed in a gradient in the second-order nucleus laminaris (NL; Person et al., 2004), and misexpression of EphA4 in chick embryos reduces tonotopic specificity by broadening projection areas to NL (Huffman and Cramer, 2007). Studies in the mouse auditory system have shown that EphA4-ephrin-B2 signaling regulates growth of spiral ganglion cell neurites in the developing ear (Brors et al., 2003), and Eph proteins influence growth of inner ear efferents from the brainstem (Cowan et al., 2000; for review see Cramer, 2005; Webber and Raz, 2006).

Whether deficits in either EphA4 or ephrin-B2 affect the functional organization of the mammalian auditory brainstem is not known. This study addresses the role of Eph proteins in the organization of frequency selectivity in the mammalian auditory brainstem using two mutant mouse strains, one deficient in the receptor EphA4 and the other deficient in ephrin-B2, one of the ligands for EphA4. We demonstrated that these proteins are expressed in the developing auditory brainstem, and we found graded expression patterns in neonates. We also exposed animals to pure tones and examined activation of *c-fos*, an immediate early gene correlated with neural activation, in wild-type mice and in mice lacking Eph proteins. After pure tone exposure, we evaluated *c-fos* activation levels and width of frequency bands in the dorsal cochlear nucleus (DCN) and the medial nucleus of the trapezoid body (MNTB), nuclei that represent components of two distinct auditory pathways. We found that the precise spatial arrangement of tone-evoked neural activation in these mammalian auditory nuclei is altered by deficiencies in these Eph family proteins.

MATERIALS AND METHODS

Animals

Ephrin-B2 mutant mice (Dravis et al., 2004) on a CD-1/129 background were bred in our colony. The mutant allele encodes a membrane-bound ephrin-B2-β-galactosidase fusion protein that lacks the cytoplasmic domain. The studies reported here compare *ephrin-B2*$^{+/+}$ with *ephrin-B2*$^{lacZ/+}$, because the homozygous ephrin-B2 mutation is lethal at P0. EphA4 gene trap mice (Leighton et al., 2001) were provided courtesy of Marc Tessier-Lavigne and were bred in our colony on a C57/Bl6 background. The mutant allele produces no EphA4 protein and expresses cytoplasmic β-galactosidase. Our studies included wild-type (*EphA4*$^{+/+}$), heterozygous (*EphA4*$^{+/-}$), and homozygous (*EphA4*$^{-/-}$) mice. All procedures were approved by the University of California Animal Care and Use Committee (IACUC).

X-gal histochemistry

Heterozygous mice were used at P3, P6, P10, and P18 for developmental expression studies. Mice were anesthetized with Isoflurane USP (Abbott Laboratories), followed by transcardial perfusion with 0.9% NaCl, followed by 4% paraformaldehyde (PFA) in 0.1 M phosphate buffer, pH 7.4. Brains were then postfixed in PFA for 15 minutes and equilibrated in 30% sucrose overnight. Within 24 hours, the brains were sectioned on a cryostat in the coronal plane at 14 μm, mounted on glass slides, and heated for at least 60 minutes on a slide warmer. Slides were rinsed in phosphate-buffered saline (PBS; pH 7.4), then incubated at 37°C in a solution containing 5 mM ferrocyanide, 5 mM ferricyanide, 2 mM MgCl, and 1 mg/ml 5-bromo-4-chloro-3-inolyl,betaD-galactopyranoside (X-gal; Sigma, St. Louis, MO) in PBS until a dark blue reaction product could be observed on the tissue. Slides were then rinsed three times in PBS and coverslipped with Glycergel mounting medium (Dako, Carpinteria, CA).

Acoustic stimulation

Awake, freely moving mice at ages P18–25 were placed on a cardboard platform with a screen cover to maximize sound at the head. The platform was placed inside an acoustically isolated sound chamber, adjacent to a speaker. Tones were controlled using MALab (Kaiser Instruments, Irvine, CA) and delivered through an electrostatic speaker (ES-1; Tucker-Davis Technologies, Gainesville, FL). Calibration was performed using a microphone (Bruel and Kjaer, Norcross, GA) in the position of the animal (Kaur et al., 2004). The platform was small enough to ensure that mice were never more than 10 cm from the speaker. Mice were kept in silence for 60 minutes, followed by free field tone pips at 75 dB SPL for 90 minutes. For some animals, sound was delivered as 8-kHz tone pips, of 50 msec duration, with a 2.5-msec rise-fall time and 40-msec gap. For another group of animals, sound was delivered as 12-, 15-, or 40-kHz tone pips, of 400 msec duration, with a 5-msec rise-fall time and 300-msec gap. Control animals were maintained in the chamber for 120 minutes in silence, with no tone presentation. Prior to tone exposure, ear canals were examined with an otoscope to confirm a clear path to the tympanic membrane.

Auditory thresholds

The CD-1/129 mouse strain does not undergo hearing loss with age. However, behavioral studies have shown age-related hearing loss after 6 weeks of age in the C57/Bl6 strain (Ouagazzal et al., 2006). The C57/Bl6 background strain shows auditory brainstem response (ABR) thresholds within the normal range between 7 and 30 postnatal weeks (Zheng et al., 1999). Thus the P18–25 age range chosen for this study falls before age-related hearing loss occurs in this strain yet shows measures of threshold and sensitivity that are comparable to those of the adult mouse (Song et al., 2006). Furthermore, the behavioral threshold for C57/Bl6 mice at older ages of 2–4 months is reported as 40 dB SPL for 40 kHz and 35 dB for 8 kHz, making the 75-dB level employed in this study of P18–25 animals well above threshold (Mikaelian et al., 1974).

Tissue processing

Within 15 minutes of the acoustic stimulation period, all mice were immediately moved to a surgical area, anesthetized with isoflurane, and perfused transcardially (described above). The brains were carefully removed from the calvarium and equilibrated overnight in 30% sucrose at 4°C, then sectioned on a cryostat in the coronal plane at 30 μm within 24 hours of sucrose embedding. Every third section was collected into a 24-well plate containing PBS and saved for c-fos immunohistochemistry. A series of adjacent sections was mounted on glass slides and stained with thionin for confirmation of anatomical boundaries.

c-fos Immunohistochemistry

The primary antibody for c-fos detection used in this study was a rabbit polyclonal manufactured by Calbiochem, EMD Biosciences (catalog No. PC-38) and was provided in the form of undiluted serum. The immunogen to create this antibody was a synthetic peptide with the amino acid sequence SGFNADYEASSSRC, corresponding to amino acid residues 4–17 of human c-fos protein. We performed Western blot analysis on mouse brainstem homogenates and found an intense band at 50–65 kD, corresponding to the expected size of the c-fos protein. In addition, we performed immunohistochemistry on mice kept in silence and found no c-fos-positive cells in the auditory nuclei (see Fig. 3B,D).

Floating sections were rinsed three times for 10 minutes each in PBS, then blocked in 0.05 M Tris and PBS containing 10% normal goat serum (NGS; Vector Laboratories, Burlingame, CA) and 0.25% cargeenan (Sigma) on an orbital shaker at room temperature. The blocking solution was replaced with a solution containing the primary antibody, diluted 1:2,000 in 5% NGS and 0.25% cargeenan in 0.1 M Tris. The plates were then incubated for 12–24 hours at 4°C on an orbital shaker. The sections were rinsed in PBS and incubated in a solution containing the biotinylated goat anti-rabbit secondary antibody (1:600; Vector Laboratories), in 5% NGS and 0.25% carageenan in 0.05 M Tris-PBS at room temperature for 90–120 minutes. The sections were then rinsed and reacted with an avidin-conjugate complex (ABC kit; Vector Laboratories) for 45 minutes. Sections were then rinsed in PBS and transferred to clean 24-well plates containing 0.1 M Tris-buffered saline. Diaminobenzidine (DAB) was prepared from liquid (Sigma) and reacted with the sections for 5–10 minutes, until characteristic punctate brown labeling appeared in auditory nuclei. Sections were mounted and dried onto glass slides, dehydrated through a series of ethanol and xylene, then coverslipped with DPX mounting medium (VWR).

Microscopic analysis

Brainstem sections were analyzed with a Zeiss Axioskop mounted with an Axiocam digital camera and OpenLab acquisition software (Improvision, Lexington MA). Nuclear boundaries were identified under darkfield microscopy and compared with adjacent thionin-stained sections. Images were corrected with background illumination subtraction in OpenLab. Image files were imported into Adobe Photoshop CS v8.0, and tools for level adjustments and dodging were used to optimize contrast and brightness and to compose and label figures. Representative cases were traced for reconstructions from Photoshop images.

Brainstems were included in the analysis if they satisfied the following criteria 1) punctate cell nucleus-specific DAB reaction product in brainstem and midbrain auditory nuclei and 2) at least five sequential sections containing immunolabeled cells in MNTB or eight sequential sections on at least one side of the brain containing immunolabeled cells in DCN.

Quantitative analysis

All microscopic and quantitative analyses were performed blind to genotype. For both DCN and MNTB, cells were counted in each section on both right and left sides. For each brain, the total number of c-fos-positive cells counted in each nucleus was divided by the total number of counted sections to get a value of mean cell number per section. In each case, the left and right sides were averaged together if they each fit the inclusion criteria described above. For DCN, the three sequential sections showing the greatest number of c-fos-positive cells were identified as the area of peak activation and were chosen for quantitative and topographic analysis. Thus, calculation of mean number of cells per section was determined by dividing the total number cells in the peak area of activation by three. As a result of more uniform numbers of c-fos-positive cells throughout all sections of MNTB, all sections immunolabeled for c-fos were included in the quantitative and topographic analysis. The calculation of the mean number of cells per section in MNTB was therefore determined by dividing the total number of cells counted by the total number of sections counted, which ranged from five to eight. All c-fos-positive cell counts were corrected by using the Abercrombie method (Abercrombie, 1946). The number of sections analyzed did not vary across genotypes.

Topographic measurements were made in OpenLab software. The position of each cell was defined as the distance (in micrometers) from either the dorsal tip of DCN or the medial edge of MNTB, normalized to the total length of the nucleus in that section. The positions of c-fos-positive cells in each section were then averaged to obtain a mean position value of c-fos-positive cells for the section. This mean position was then averaged over all sections in each brain to obtain a mean position value for each brain. The standard deviation of this position variable in each section was also used as an indication of tonotopic spread. All tabulated data for each brain were

then exported to JMP software (SAS Institute) for statistical comparisons of genotype groups.

PCR and genotyping

The genotype of each animal was determined by PCR. Tail samples (2 mm) were obtained from each animal prior to sound exposure and later compared with another sample taken immediately prior to transcardial perfusion. Each tail sample was digested overnight at 37°C in Eppendorf tubes containing 4 μg/ml proteinase K (Sigma) in lysis buffer (100 mM Tris-HCl, 5 mM EDTA, 0.2% SDS, 200 mM NaCl). The DNA was then extracted with 100% isopropanol and resuspended in distilled water to 0.3 μg/ml. PCR amplification of *EphA4* was performed with three oligonucleotides containing the sequences GTTTCCGCTCTGAGCTTATACTGC, ACAGTGAGTGGACAAAGAGACAGG, and CGCTCTTACCAAAGGGCAAAC. Gel electrophoresis of PCR product revealed a 639-bp band for wild-type *EphA4* DNA and an 800-bp band for the mutant allele. Ephrin-B2 PCR genotyping was performed with three oligonucleotides containing the sequences AGGCGATTAAGTTGGGTAACG, TCTGTCAAGTTCGCTCTGAGG, and CTTGTAGTAAATGTTGGCAGGACT (Operon Biotechnologies, Huntsville, AL). Gel electrophoresis of PCR product revealed a 500-bp band for wild-type *ephrin-B2* DNA and a 400-bp band for the mutant lac-Z containing *ephrin-B2* allele, as described for this mouse line (Dravis et al., 2004).

RESULTS

Spatiotemporal patterns of EphA4 in auditory nuclei

To assess the role(s) of Eph proteins in the functional organization of auditory pathways, we first examined expression patterns of EphA4 during the postnatal period. We used X-gal histochemistry to detect β-galactosidase expression in an *EphA4* mutant line with inserted lacZ sequences that faithfully report EphA4 expression (Leighton et al., 2001). Within the ventral cochlear nucleus (VCN), EphA4 expression at P3 is graded, with highest levels in the dorsalmost, high-frequency quadrant of the principal cell area. The granular cell area in the lateral portion of the VCN is thick at this early postnatal age and shows no staining (Fig. 1A). From P10 to P18, EphA4 has a more uniform expression pattern in the VCN; an example of expression at P18 is shown in Figure 1B. Similarly, a high- to low-frequency gradient of expression was seen in DCN at P3 (Fig. 1C), and expression became more uniform across the frequency axis at later ages (Fig. 1D). X-gal labeling showed uniform expression across the frequency axis of MNTB at P3 (Fig. 1E) and later ages (Fig. 1F), consistent with our previous observations in this nucleus (Hsieh et al., 2007). EphA4 is also expressed in a high- to low-frequency gradient in the central nucleus of the inferior colliculus (cIC; Fig. 1G), and expression becomes more uniform at P18 (Fig. 1H).

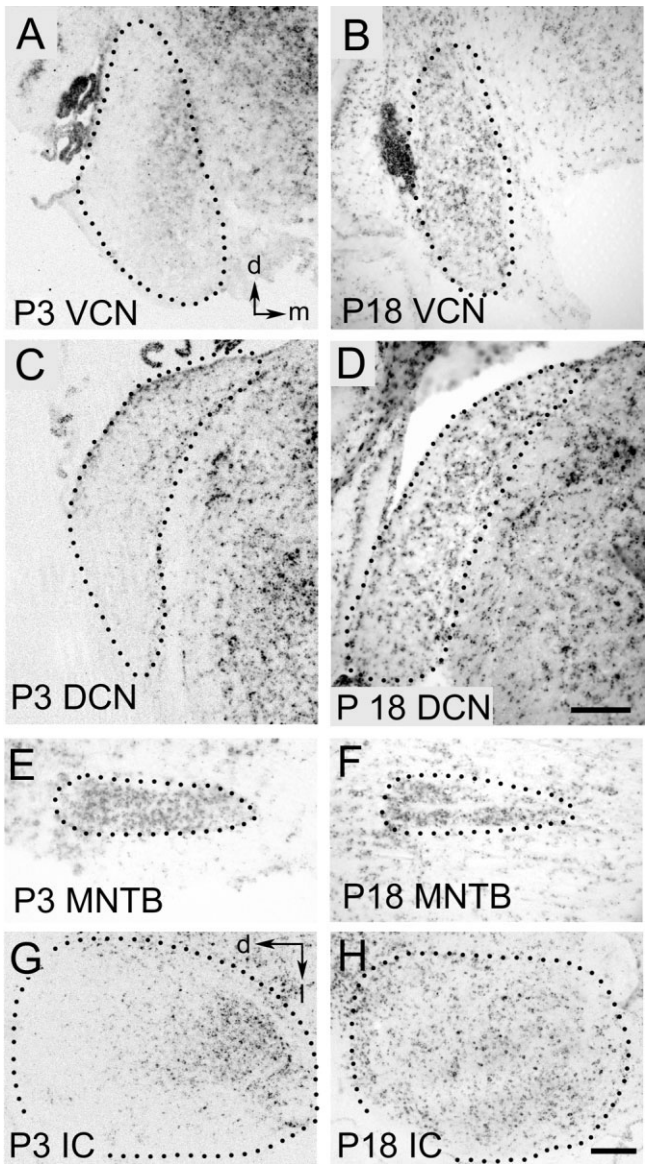

Fig. 1. Expression of EphA4 in auditory nuclei. **A:** *EphA4*$^{+/-}$ mice were used for X-gal histochemistry to report EphA4 expression. VCN is outlined in dotted lines (including principal cells and the granular layer). At P3, label is seen in a gradient with dorsal (high-frequency) region showing more pronounced expression in the principal cells. The thick granular layer shows no expression. Axes indicate dorsal and medial for A–F. **B:** P18 VCN shows label throughout the nucleus, and the gradient is no longer apparent. **C:** At P3, the DCN shows a gradient similar to that of P3 VCN, with expression in dorsal regions higher than ventral regions. **D:** P18 mouse shows uniform EphA4 expression along the frequency axis of DCN. **E:** EphA4 is uniformly expressed along the mediolateral frequency axis of MNTB. **F:** At P18, expression remains and does not vary along the mediolateral axis. **G:** At P3, EphA4 is expressed in a gradient across the frequency axis of the inferior colliculus (IC). Axes indicate dorsal and lateral for G,H. **H:** At P18, labeling in the IC is more evenly distributed. Scale bars = 100 μm in D (applies to A–D); 100 μm in H (applies to E–H).

Spatiotemporal patterns of ephrin-B2 in auditory nuclei

To characterize the developmental expression of ephrin-B2 in the auditory pathway, we used *ephrin-B2*$^{lacZ/+}$ mice in which the mutant gene encodes a membrane-bound ephrin-B2-β-galactosidase fusion protein (Dravis et al., 2004). We found that ephrin-B2 is heavily expressed in the auditory nerve at P3 in the portion of the nerve near the brainstem entry (Fig. 2A). The

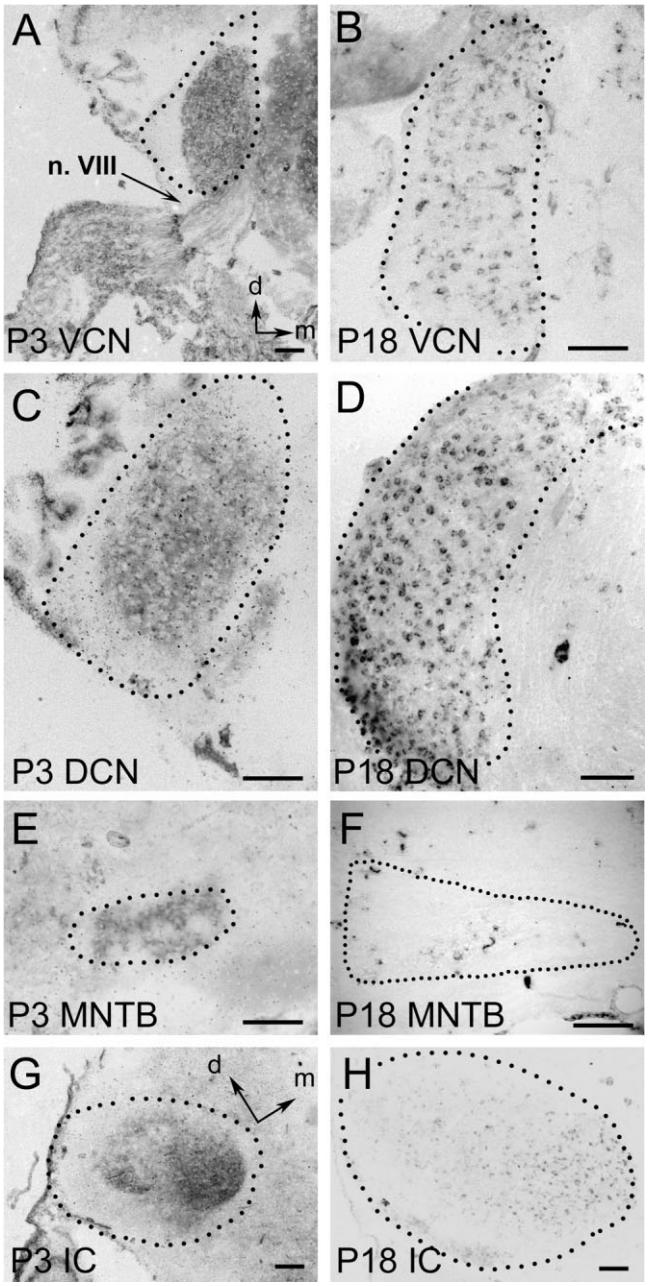

Fig. 2. Expression of ephrin-B2 in auditory nuclei. **A:** *Ephrin-B2*$^{lacZ/+}$ mice were used to report ephrin-B2 expression. Labeling is distributed throughout VCN at P3. In addition, axons in the VIIIth nerve (n. VIII) express ephrin-B2 in a nonuniform manner. Axes indicate dorsal and medial for A–F. **B:** Labeling is uniform throughout the frequency axis of VCN at P18. **C:** In DCN, label is diffuse at P3 and excludes the granule cell layer. **D:** Uniform expression persists in DCN at P18. **E:** At P3, MNTB has uniform label across the lateromedial axis. **F:** MNTB has no detectable ephrin-B2 expression at P18. **G:** The central region of IC expresses ephrin-B2 in a ventral-to-dorsal gradient at P3. Axes apply to G,H. **H:** Expression in IC is reduced at P18 but is still expressed in a ventral-to-dorsal gradient. Scale bars = 100 μm.

pattern of expression is nonuniform and is reduced in the nerve at P10 (data not shown). Unlike that of EphA4, ephrin-B2 expression is uniform along the dorsoventral frequency axis of the VCN at P3 (Fig. 2A) and remains uniform at P18 (Fig. 2B). Expression is also uniform in the DCN at both ages (Fig. 2C,D). As with EphA4, ephrin-B2 shows no apparent gradient along the mediolateral frequency axis of MNTB at P3 (Fig. 2E), and at P18 expression is nearly absent (Fig. 2F). Additionally, ephrin-B2 has a distribution similar to that of EphA4 in the cIC, where it is expressed in a high- to low-frequency gradient at P3 (Fig. 2G), yet, unlike the case with EphA4, graded expression persists at P18 (Fig. 2H). Together, these results show that gradients of expression of EphA4 and ephrin-B2 are present in subcortical auditory nuclei during the formation of auditory connections.

Evaluation of frequency selective bands in wild-type mice

The expression patterns in the auditory nuclei at early ages suggest that EphA4 and ephrin-B2 may be involved in formation of tonotopic projections in two distinct pathways. The VCN projects to the superior olivary complex, which includes MNTB, via the ventral acoustic stria. The DCN projects directly to the contralateral inferior colliculus and contralateral cochlear nucleus through the dorsal acoustic stria (Cant and Benson, 2003).

We followed c-fos expression after pure tone exposure to evaluate frequency-specific activation patterns in auditory brainstems of mutant mice. To identify auditory nuclei suitable for this analysis, we first established which nuclei in wild-type animals showed consistent frequency bands of c-fos-positive cells after pure tone exposure. Several studies have demonstrated that the position of bands of c-fos-positive neurons varies with the frequency of the stimulus in the auditory brainstem nuclei, and the positions correlate with physiologically identified isofrequency axes (Ehret and Fischer, 1991; Friauf, 1992; Rouiller et al., 1992; Brown and Liu, 1995; Saint Marie et al., 1999a,b). Because the conditions and species varied in these studies, we had first to establish optimal, consistent frequency bands in auditory nuclei of wild-type mice before comparing distributions of cell activation with those seen in mutant mice.

After tone exposure and c-fos immunohistochemistry, we examined the distribution of labeled cells in several nuclei. Figure 3 shows representative examples of the labeling patterns observed under our conditions. In the DCN (Fig. 3A), a cluster of labeled cells was consistently observed after exposure to 8-kHz pure tones. Animals maintained in silence showed very little c-fos expression in DCN (Fig. 3B). This 8-kHz pure tone was the optimal frequency for obtaining consistent bands in this nucleus, because with responses obtained with higher frequencies it was difficult to distinguish the band from the granule cell cap activation. Clusters of labeled cells were seen in appropriate frequency areas within MNTB using 40-kHz pure tone stimulation (Fig. 3C), although not in animals maintained in silence (Fig. 3D) and not in animals exposed to lower frequency tones (not shown). For the VCN (Fig. 3E), we did not observe clusters or bands of labeled cells like those in DCN; activation was diffuse along the dorsoventral axis. This result is consistent with previous studies using similar methods (Ehret and Fischer, 1991). For both low and high frequencies, we did not consistently observe labeled cells in discrete frequency bands in the IC that were distinguishable from off-band activation (Fig. 3F). Analysis in the remainder of the study thus focused

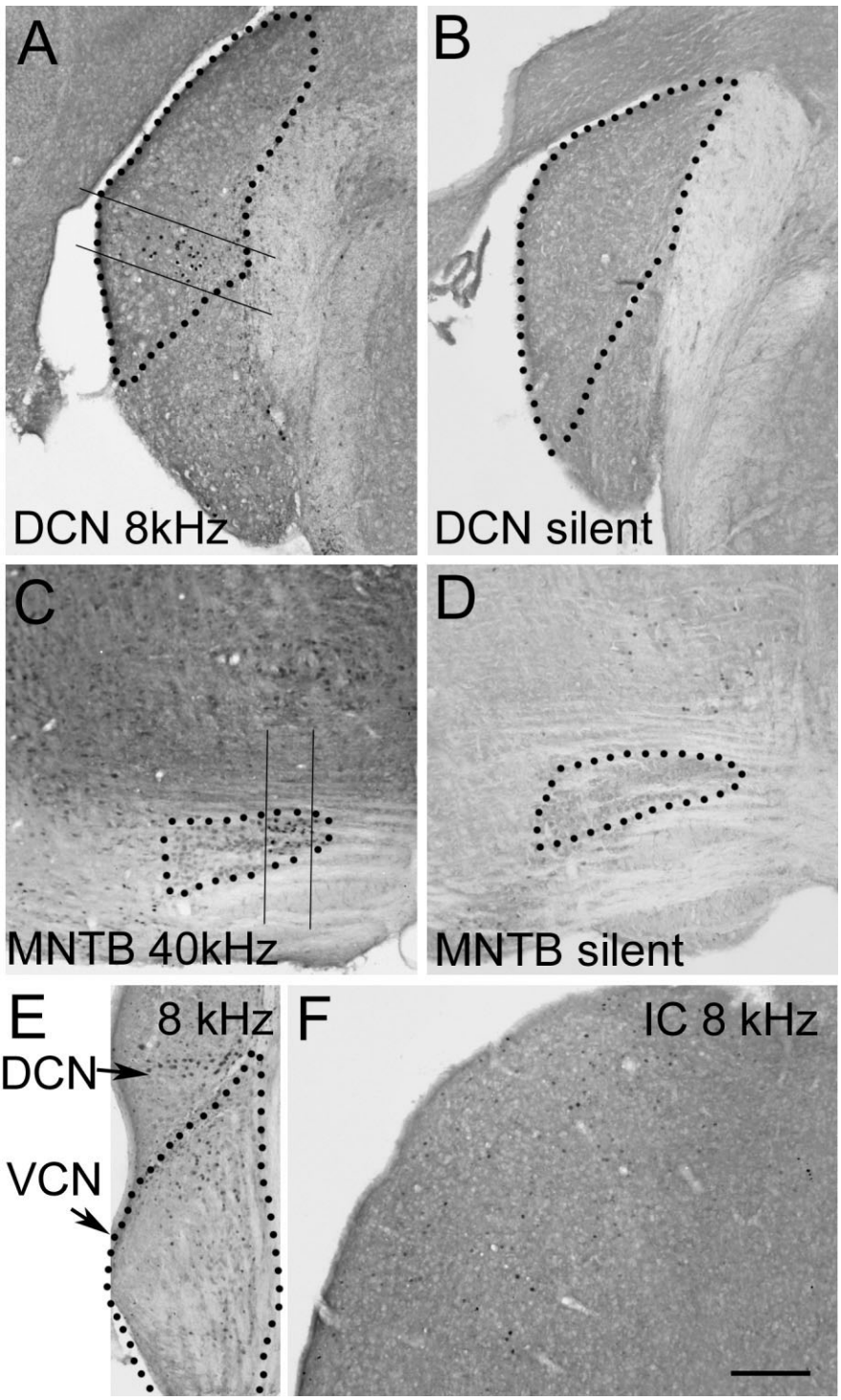

Fig. 3. Summary of c-fos patterns in auditory nuclei in wild-type mice. In all panels, medial is to the right and dorsal is upward. **A:** DCN showed consistent bands of c-fos-positive cells in response to 8-kHz stimulation (black lines). **B:** Labeled cells were not seen in tissue from animals maintained in silence. **C:** MNTB consistently had clustered bands of c-fos-positive cells in response to the 40-kHz stimulus. **D:** MNTB showed no c-fos-positive cells in animals maintained in silence. **E:** c-fos immunolabeling in VCN (dotted outline) was diffuse and variable in response to 8-kHz, whereas DCN (partially visible above VCN) showed a recognizable cluster. **F:** c-fos responses were highly variable in IC for both 8- and 40-kHz tones. In this representative example, a small number of widely spaced c-fos-positive cells are seen in response to the 8-kHz stimulus. Scale bar = 100 μm, applies to all panels.

on 8-kHz tone exposure to examine the DCN and 40-kHz tone exposure to examine the MNTB. These two nuclei are the lowest-order nuclei in the two pathways through the dorsal and ventral acoustic striae, respectively, for which we obtained robust frequency bands in wild-type animals.

c-fos Immunoreactivity in DCN after exposure to 8-kHz tones

After exposure to 8-kHz pure tones, the cluster of c-fos-positive cells was typically seen in the low-frequency, ventral half of DCN. These c-fos-positive cells formed a mediolateral band, transverse to the longer dorsoventral dimension of the nucleus. Figure 4A shows a discrete band of labeled cells in DCN of an $EphA4^{+/+}$ mouse brainstem. In $EphA4^{-/-}$ DCN, there was a 42% reduction in the mean number of c-fos-positive cells/section (14.9 ± 1.7; n = 3) compared with wild-type DCN (25.7 ± 2.1 n = 3; $P < 0.05$, *t*-test; Fig. 5, upper left). The spread of activation (standard deviation of mean position) did not differ between these groups ($EphA4^{+/+}$ 0.066 ± 0.035 vs. $EphA4^{-/-}$ 0.087 ± 0.022, $P > 0.6$, ANOVA), suggesting that, although there are fewer c-fos-positive cells activated in $EphA4^{-/-}$ mice in response to a pure tone stimulus, these cells have a distribution along the tonotopic axis similar to that seen in wild-type mice (Fig. 5, upper right).

In contrast to this difference in the number of c-fos-positive cells, DCN in *ephrin-B2*$^{+/+}$ and *ephrin-B2*$^{lacZ/+}$ mice showed no difference in the number of c-fos-positive cells in response to 8 kHz pure tone exposure (*ephrin-B2*$^{+/+}$ 29.5 ± 7.7; n = 3 vs. *ephrin-B2*$^{lacZ/+}$ 30.0 ± 6.9 cells/section; n = 5; $P > 0.9$, *t*-test; Fig. 5, lower left). However, in an analysis of dorsoventral spread, we found that the standard deviation of position was significantly larger in *ephrin-B2*$^{lacZ/+}$ mice (0.144 ± 0.005) than wild-type controls (0.106 ± 0.012; $P < 0.02$, *t*-test; Fig. 5, lower right). All c-fos-positive cell counts were adjusted by correction factors for nuclear size (Abercrombie, 1946), and no significant differences in nuclear size were observed between genotypes for either DCN or MNTB.

c-fos-Positive cells in MNTB after exposure to 40-kHz tones

After exposure to 40-kHz tones, the c-fos-positive cells in MNTB formed a discrete band in the medial half of the nucleus. The immunoreactive cells were arranged in a banded cluster, transverse to the mediolateral, tonotopic axis (Fig. 6). An example of labeling in an $EphA4^{+/+}$ mouse brainstem is shown in Figure 6A. $EphA4^{-/-}$ mice had fewer cells in each band than matched wild-type controls (Fig. 6B). Similarly, bands of c-fos-positive cells after pure tone exposure in *ephrin-B2*$^{lacZ/+}$ mice (Fig. 6D) contained fewer cells than those seen in *ephrin-B2*$^{+/+}$ mice (Fig. 6C). Traced reconstructions of sections through MNTB show the appearance of c-fos-positive bands in representative wild-type and $EphA4^{-/-}$ cases and illustrate changes in cell number and position (Fig. 6E).

Quantification of number and position of these c-fos-positive cells in MNTB showed significant differences among genotype groups. The number of c-fos-positive cells per section in $EphA4^{-/-}$ (2.77 ± 0.47) and $EphA4^{+/-}$ (2.95 ± 0.81) mice were both significantly reduced compared with wild-type controls (6.86 ± 1.30; $P < 0.05$, ANOVA; Fig. 7A, left). The standard deviation of position across the tonotopic axis was significantly smaller in both $EphA4^{-/-}$ mice (0.063 ± 0.011) and $EphA4^{+/-}$ (0.070 ± 0.007) than in wild-type controls (0.094 ± 0.003; $P < 0.05$, ANOVA; Fig. 7A, right). These MNTB results suggest a reduction of cell number activation similar to that seen in DCN and, furthermore, that the tonotopic spread is narrower in $EphA4^{-/-}$ and $EphA4^{+/-}$ mice than in wild-type controls. In *ephrin-B2*$^{lacZ/+}$ mice, the number of c-fos-positive cells per section (3.26 ± 0.63) was also significantly reduced compared with wild-type controls (6.12 ± 0.72; $P < 0.05$, *t*-test; Fig. 7B, left). However, the standard deviation of position was not significantly different ($P > 0.2$) from that in wild-type controls (Fig. 7B, right). These results suggest that ephrin-B2 has a role in MNTB different from that in DCN.

The mean position of each band in MNTB was more lateral in $EphA4^{+/-}$ and $EphA4^{-/-}$ mice than in wild-type controls (Fig. 7C). As a percentage of the mediolateral extent, wild-type mice showed that the mean position of labeled cells was centered at 26.8% ± 1.5% of the nucleus. In heterozygotes, this mean position was centered at 36.0% ± 3.5%, and, in $EphA4^{-/-}$ mice, it was 36.6% ± 2.7%. Both heterozygotes and mutants differed significantly from wild types in this mean position measurement ($P < 0.05$, ANOVA). In *ephrin-B2*$^{lacZ/+}$ mice, the mean position was not statistically significantly different from wild-type littermate controls ($P > 0.5$, *t*-test). These results suggest that reduction *or* deletion of EphA4 shifts the normal tonotopic arrangement in MNTB, whereas reduction of ephrin-B2 does not.

DISCUSSION

The present study examines how mutations in *EphA4* and *ephrin-B2* affect patterns of neural activation in the auditory brainstem. We demonstrated the presence of reporters for both EphA4 and ephrin-B2 proteins in auditory brainstem nuclei during early postnatal development (P3) and at a posthearing-onset period of P18–25. We found that, at P3, ephrin-B2 shows a nonuniform expression pattern in the VIIIth nerve and that EphA4 is expressed in a high- to low-frequency gradient in both DCN and VCN. Furthermore, both molecules show a graded expression pattern in the inferior colliculus; this pattern becomes more uniform for EphA4, but not for ephrin-B2. These expression data motivated our analysis of functional activation patterns in mutant mice.

To examine how the loss of Eph family proteins influences the functional organization of cells in these auditory nuclei, we first identified nuclei that gave a robust, consistent band of c-fos-positive cells in response to pure tones in wild-type mice. We found a consistent banded pattern only in DCN and in MNTB, which represent components of distinct auditory pathways. We then compared these patterns with those we obtained in mutant mice. Our results are summarized in Figure 8. In EphA4 mutant mice, fewer cells were c-fos positive in both nuclei, and these cells were more narrowly distributed in MNTB. The position of this narrowed band was also shifted laterally within MNTB. In *ephrin-B2* heterozygous mice, c-fos-positive cells were more broadly distributed in DCN and were less numerous in MNTB. Taken together, our results provide the first evidence that Eph proteins have important roles in the tonotopic organization of mammalian auditory brainstem nuclei.

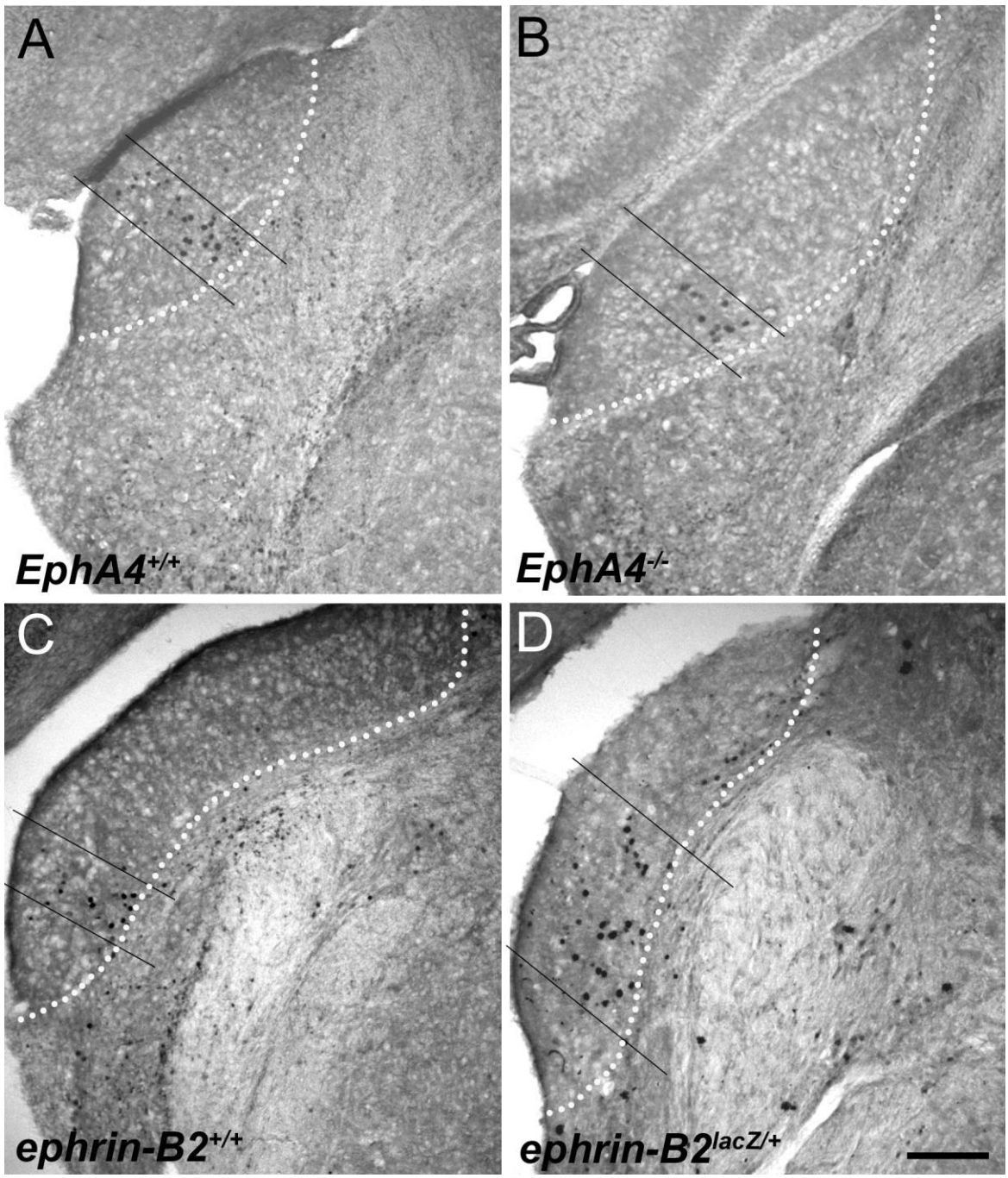

Fig. 4. Coronal sections showing c-fos immunoreactivity in DCN after exposure to 8-kHz pure tones. In all panels, medial is to the right and dorsal is upward. **A:** *EphA4*$^{+/+}$ mice show a discrete band of c-fos-positive cells toward the ventral region of DCN, outlined in dotted lines. **B:** In *EphA4*$^{-/-}$ mice, c-fos immunoreactivity was still restricted to a discrete band, but fewer cells were labeled. **C:** *Ephrin-B2*$^{+/+}$ mice show a band of c-fos-positive cells in response to pure tone stimulation. **D:** *Ephrin-B2*$^{lacZ/+}$ mice show a broader distribution of c-fos-positive cells in response to the 8-kHz tone. The elongated appearance of DCN in C and D (compared with A and B) reflects a more caudal pair of sections through the nucleus and a slight difference in morphology in the two background strains that does not result from the mutation. Scale bar = 100 μm.

Measures of auditory activation with c-fos

Our measure of neural activation reflects neurotransmission from afferent to target that causes action potential generation, calcium influx, and subsequent rapid transcription of the immediate early gene *c-fos* (Morgan and Curran, 1989; Kovacs, 1998). This measure allows detection of suprathreshold excitatory events, which re-

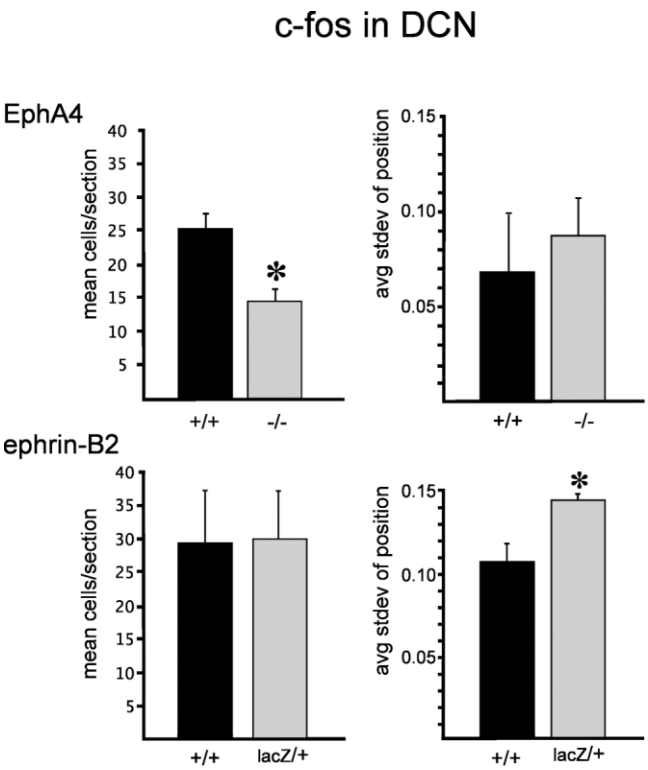

Fig. 5. Quantification of the number and spread of c-fos-positive cells in DCN after exposure to 8-kHz pure tones in two mouse lines. Error bars denote standard errors of the mean in this and all other figures. Asterisks indicate statistically significant differences using Student's *t*-test. Top: In *EphA4*$^{-/-}$ mice (n = 3), there were significantly fewer c-fos immunoreactive cells in DCN than in *EphA4*$^{+/+}$ mice (n = 3; *$P < 0.05$), but the spread, measured as the standard deviation of position, was not significantly different between these two genotypes. Bottom: *Ephrin-B2*$^{+/+}$ mice (n = 3) and *ephrin-B2*$^{lacZ/+}$ mice (n = 5) had similar numbers of c-fos-positive cells in DCN, but the spread was significantly greater in *ephrin-B2*$^{lacZ/+}$ mice than in wild-type mice (*$P < 0.05$).

sult from the summed inputs to each cell. Firing rates of labeled cells are not distinguishable; hence, this method does not provide information about tuning curves for individual neurons. However, c-fos immunoreactivity arises in cells that contain the stimulus frequency within their excitatory receptive fields. We thus focused on the spatial distribution of those cells, a reflection of the tonotopic order.

DCN and MNTB consistently showed frequency-specific expression bands of c-fos-positive cells here and in previous studies (Ehret and Fischer, 1991; Rouiller et al., 1992; Brown and Liu, 1995). Within the cochlear nucleus, DCN has shown a more consistent tonotopic expression of c-fos protein than VCN. The lack of consistent tonotopic bands in VCN may be due in part to the relatively high level of spontaneous activity in this nucleus (Woolf and Ryan, 1985), which would undermine the recognition of a distinct tone-evoked band, as suggested in Figure 3E. Moreover, differential expression of c-fos protein in the anterior and posterior divisions of VCN might compromise recognition of distinct bands along the rostrocaudal extent of our tissue sample. Furthermore, the requirement of high intensities (120 dB) to recruit tonotopic c-fos mRNA (Saint Marie et al., 1999a; Yang et al., 2005) suggests that c-fos expression in this nucleus is not sensitive to the 75-dB stimulus levels used in this study. However, expression of c-fos mRNA does correlate with stimulus frequency in MNTB (Saint Marie et al., 1999a), and our 40-kHz, 75-dB stimulus was also effective at recruiting a spatially restricted frequency band of c-fos protein expression in this nucleus. The superior efficacy of 40 kHz over lower frequencies reflects the role of MNTB in processing high-frequency stimuli within the interaural level difference pathway. Taken together, our study and previous studies support the use of c-fos as a consistent assay for frequency organization in DCN and MNTB.

Differences in c-fos-positive cell number

The number and pattern of c-fos-positive cells in response to pure tone stimulation were altered in the mutant mice. Changes were observed in EphA4 and ephrin-B2 mutant mice in auditory nuclei that express these proteins. However, because the mutant mice lack the genes in all cells, we cannot say with certainty that the changes are due to loss of proteins in these nuclei. Indirect effects downstream of deficits in earlier development remain possible.

Lack of EphA4 influences the magnitude of activation in both the DCN and the MNTB, whereas reduction of ephrin-B2 affects magnitude only in MNTB. One of the reasons for this difference could be a stronger impact of EphA4 receptor loss on the ear than in the central nervous system. EphA4 repels both ephrin-B2- and ephrin-B3-containing spiral ganglion neurites (Brors et al., 2003). Hence, one possibility is that mistargeted primary afferents in the ear of *EphA4*$^{-/-}$ mice might be deficient in connections to the brainstem, which results in reduced tone-evoked activation. In contrast, the lack of effect on magnitude in *ephrin-B2*$^{lacZ/+}$ DCN suggests that a single copy of the wild-type *ephrin-B2* allele may be sufficient for normal activation in the cochlea and DCN. Our analysis was restricted to heterozygous *ephrin-B2* mice, because homozygous mutations are lethal at about P0. The specific effect on topographic activation in the DCN of *ephrin-B2*$^{lacZ/+}$ mice without an effect on magnitude suggests that ephrin-B2 protein is an important local cue for correct targeting in the developing central nervous system.

Differences in tonotopic distribution in DCN and MNTB

Effects of Eph or ephrin mutations on the width or position of bands of c-fos-positive neurons might arise from targeting errors in the tonotopic projections to auditory brainstem nuclei. The presence of ephrin-B2 in the auditory nerve and the gradient of EphA4 along the frequency axis in DCN at early postnatal ages provide one possible combination of proteins that can guide topography in this nucleus. These expression patterns are observed at P3, a time that precedes the elaboration of axon terminals and formation of synapses in the hamster DCN (Schweitzer and Cant, 1984). Our data thus support a role for these proteins in axon guidance. That DCN shows topographic errors in *ephrin-B2*$^{lacZ/+}$ mice but not in *EphA4*$^{-/-}$ mice suggests that partial loss of this ligand has a greater effect on topography than loss of the receptor.

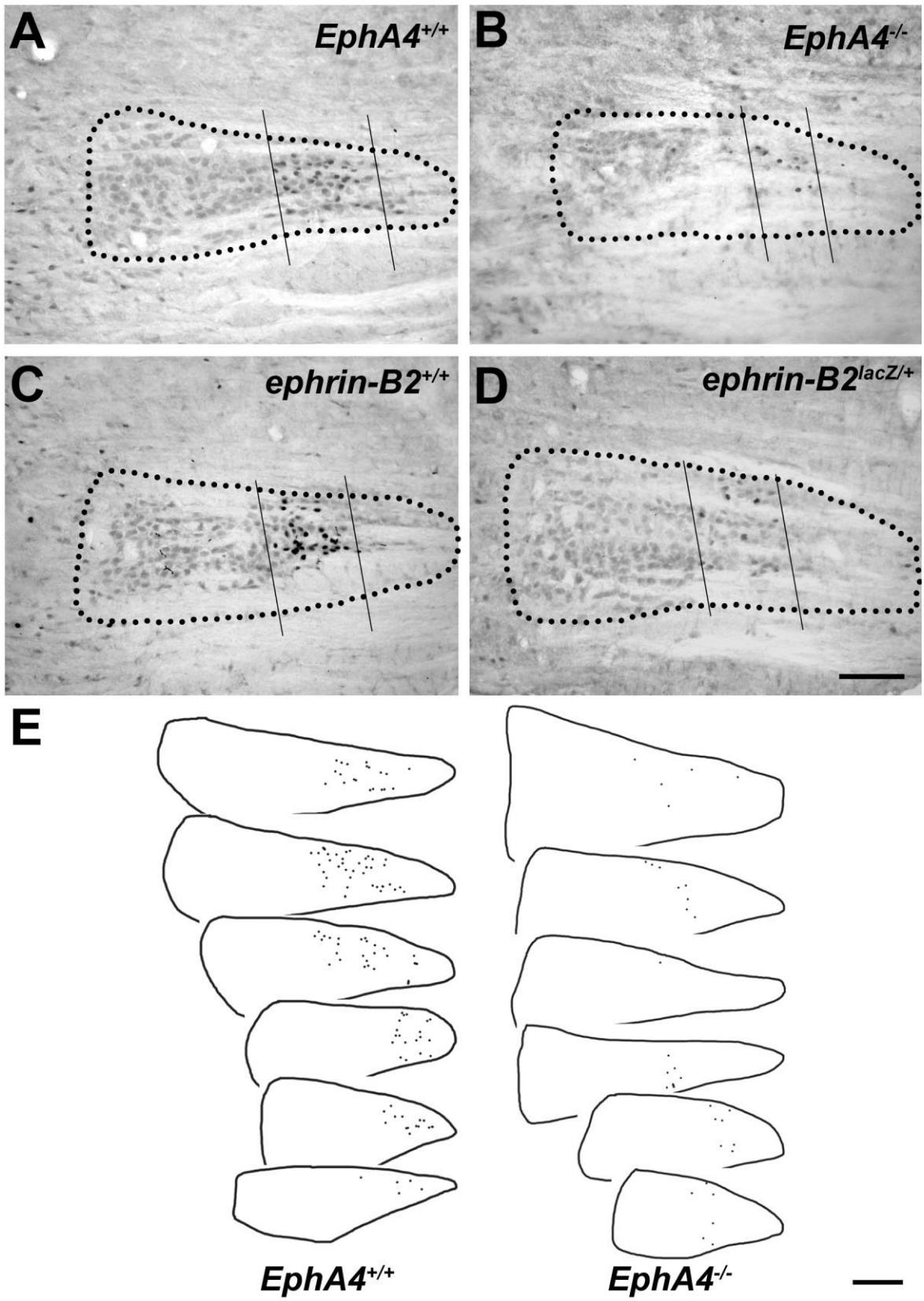

Fig. 6. Coronal sections showing c-fos immunoreactivity in MNTB following exposure to 40-kHz pure tones. In all panels, medial is to the right and dorsal is upward. MNTB is outlined in all panels with black dots. **A:** *EphA4*$^{+/+}$ mice have a distinct band of c-fos-positive cells in the medial (high frequency) region of MNTB. B. In *EphA4*$^{-/-}$ mice, c-fos immunoreactivity was restricted to a significantly narrower band than in wild-type mice. Additionally, fewer cells were c-fos-positive. **C:** In *ephrin-B2*$^{+/+}$ mice, there was also a distinct band of c-fos-positive cells in MNTB in response to pure tone stimulation. **D:** *Ephrin-B2*$^{lacZ/+}$ mice had significantly fewer c-fos-positive immunoreactive cells in MNTB than did wild-type mice ($P < 0.02$, *t*-test). **E:** Reconstructions of representative examples of *EphA4*$^{+/+}$ (left) and *EphA4*$^{-/-}$ (right) MNTB showing the entire rostrocaudal extent of the nucleus with medial edges aligned, and each dot representing a single c-fos-positive cell. There are fewer c-fos-positive cells in *EphA4*$^{-/-}$ mice, especially in the medial portion of the nucleus. The labeled cells are more narrowly distributed. Scale bars = 100 μm in D (applies to A–D); 100 μm in E.

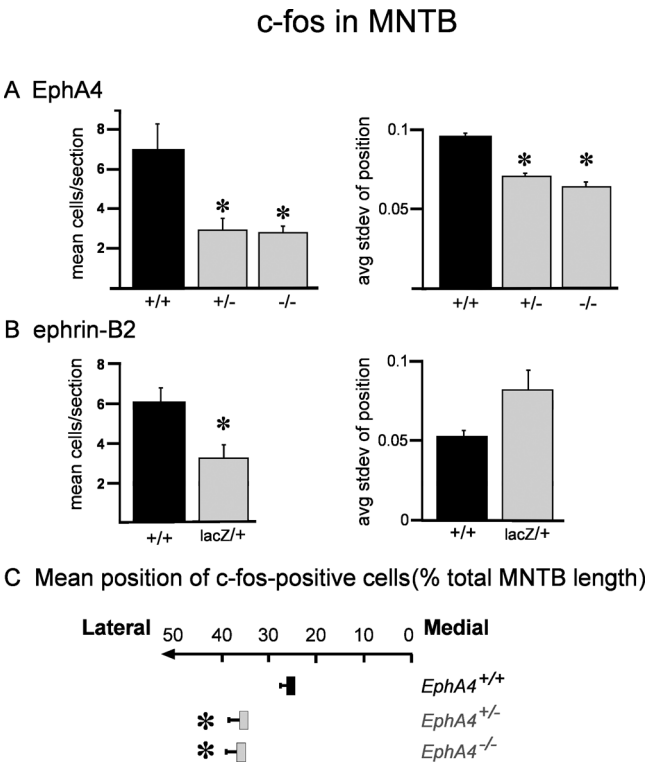

Fig. 7. Quantification of the number and spread of c-fos-positive cells in MNTB after 40-kHz pure tone stimulation. **A:** *EphA4*$^{+/+}$ mice (black bar, n = 5) had a significantly greater number of c-fos-positive cells in MNTB than either *EphA4*$^{+/-}$ mice (n = 4) or *EphA4*$^{-/-}$ mice (n = 3; *$P < 0.02$, ANOVA). In addition, the mean mediolateral spread, taken as the average standard deviation of position, was significantly smaller in both *EphA4*$^{+/-}$ mice and *EphA4*$^{-/-}$ mice than in *EphA4*$^{+/+}$ mice (*$P < 0.03$), indicating that stimulation of the nucleus with pure tones activates cells in a more narrow topographic region. **B:** *Ephrin-B2*$^{+/+}$ mice (black bar, n = 4) had a significantly greater number of c-fos-positive cells in response to the pure tone stimulation than *ephrin-B2*$^{lacZ/+}$ mice (n = 5; *$P < 0.05$). There was no significant difference in the mean standard deviation of position for these two groups of mice. **C:** Mutations in *EphA4* result in a shift of the 40-kHz frequency band in MNTB. The mean position along the mediolateral axis is plotted as a percentage of the distance along the nucleus for the same animals shown in Figure 7, top row. The mean position in *EphA4*$^{+/+}$ mice was centered at 26.8% ± 1.5% of the nucleus (black bar). This value differed from the mean position for *EphA4*$^{+/-}$ mice (36.0% ± 3.5%) and the mean position for *EphA4*$^{-/-}$ mice (36.6% ± 2.7%; *$P < 0.04$). This apparent lateral shift in the 40-kHz frequency band may arise because fewer cells are activated in the medial end of the nucleus.

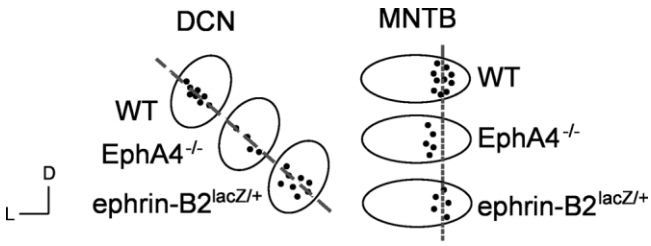

Fig. 8. Summary diagram of the results for mutations in both DCN and MNTB. Dashed lines indicate expected position of the frequency band, as observed in wild-type mice. Deletion of EphA4 results in a decreased activation of *c-fos* in both DCN and MNTB (fewer dots). The frequency band is narrower and has a laterally shifted mean position in MNTB. Reduction of ephrin-B2 results in a broader frequency band in DCN, suggesting a degradation of the tonotopic specificity in that nucleus. In addition, *ephrin-B2*$^{lacZ/+}$ mice have fewer c-fos-positive cells in MNTB after pure tone stimulation.

The effects of mutations that we observed in MNTB may similarly involve defects in axon guidance. Our expression studies demonstrate a gradient of EphA4 in VCN at P3, a time when tonotopically ordered connections from this nucleus are contacting MNTB neurons and forming calyceal synapses (Kil et al., 1995; Hoffpauir et al., 2006). The gradient of EphA4 in VCN cells may influence axon target choice along the frequency axis of MNTB during the early postnatal period. Neither EphA4 nor ephrin-B2 had graded expression in MNTB, but it remains possible that other ephrins that bind EphA4 are expressed in tonotopic gradients in MNTB.

Effects on the organization of functional activation in cerebral cortex have been demonstrated in mice lacking Eph proteins (Prakash et al., 2000; Cang et al., 2005), and these likely arise from errors in topographic mapping observed at subcortical levels (Feldheim et al., 2000; Yates et al., 2001; Dufour et al., 2003; Garel and Rubenstein, 2004). Axon targeting errors result in broadened tonotopic mapping in the chick auditory brainstem after misexpression of EphA4 (Huffman and Cramer, 2007). Thus, a broad band of cells expressing c-fos in response to a given frequency may signify that a broad region of cells receives input from neurons tuned to that frequency. Conversely, the narrowed frequency band in *EphA4*$^{-/-}$ MNTB might arise from narrowed topographic projections to MNTB. Because Eph signaling has both attractive and repulsive influences during axon guidance (Cowan and Henkemeyer, 2002; Holmberg and Frisen, 2002; Mann et al., 2004; Marquardt et al., 2005), it remains possible that they serve to either restrict or broaden projections.

An alternative explanation for the narrowed band in MNTB of EphA4 mutants relates to the reduction in the activation of c-fos-positive cells. The extent of c-fos activation within an auditory brainstem nucleus has been shown to depend strongly on the intensity of the sound presentation (Saint Marie et al., 1999a,b). Thus, an increase in the sensitivity of auditory neurons could result in an increase in the proportion of the nucleus that expresses c-fos in response to a pure tone. We used relatively low levels of sound in this study (75 dB, free field) to minimize the activation of inputs across frequencies and in accordance with previous studies demonstrating clear frequency bands (Ehret and Fischer, 1991; Friauf, 1992, 1995; Sato et al., 1993; Brown and Liu, 1995; Saint Marie et al., 1999a,b; Yang et al., 2005). Increasing neuronal sensitivity might increase the width of a frequency band. Mutations in EphA4 likely resulted in decreased sensitivity, insofar as fewer neurons expressed c-fos in these animals, but mutations in ephrin-B2 resulted in a broadened DCN frequency band, with no concurrent effect on magnitude. Changes in sensitivity are thus unlikely to account for broadening of the frequency band in *ephrin-B2* mutant DCN.

However, in MNTB, mutations in *EphA4* decreased the total number of c-fos-positive cells and also *decreased* the topographic spread of these cells. Thus, at least in this case, the effect of the mutation on c-fos-positive cell number could be related to the decreased width of the fre-

quency band. However, the change in the frequency band of *EphA4*$^{-/-}$ MNTB also included a shift to a more lateral mean position in the nucleus. This shift cannot be explained by a decrease in c-fos response alone, unless that decrease is biased toward high frequencies, represented in the medial portion of the nucleus. Thus, selective reduction of sensitivity in medial MNTB may account, at least in part, for the lateral shift of frequency bands in MNTB.

As ephrin-B2 affects spatial distribution only in DCN and magnitude only in MNTB, the role of ephrin-B2 is likely different in the cochlear nucleus than it is in MNTB. This difference in the function of ephrin-B2 may arise from variations in expression levels of this protein (Figs. 1, 2) or differences in the levels of other Eph family proteins in these structures. Although individual Eph proteins and signaling mechanisms may vary across nuclei, these gradients are consistent with a broad role for Eph family proteins in the establishment of tonotopic connections. Moreover, the gradients of EphA4 and ephrin-B2 that we observed in the IC suggest that these proteins might have a similar role in the auditory midbrain as well.

Impact of Eph family proteins on neural circuitry

This study provides evidence that EphA4 and ephrin-B2 participate in forming the functional organization of frequency responses in the auditory brainstem. Our expression studies are consistent with a role for axon pathfinding. Although axon targeting errors may account for the broadening of the frequency band in DCN, other functions of Eph proteins may underlie these changes. Interactions between ephrins and Eph receptors mediate dendritic spine formation in hippocampus (Murai et al., 2003), synapse formation (Rodenas-Ruano et al., 2006), and physiologically measured synaptic plasticity (Grunwald et al., 2004). These studies likely generalize to the auditory brainstem nuclei, where Eph proteins may contribute to complex aspects of network organization, including the strengths of individual synapses. Moreover, other Eph proteins may interact with EphA4 and ephrin-B2 during development. Thus there are several functions for Eph proteins that may result in altered functional topography in the auditory brainstem, and multiple functions may act at early stages of this pathway.

ACKNOWLEDGMENTS

We are grateful to Marc Tessier-Lavigne for providing the *EphA4* mutant mouse line. We thank Raju Metherate for the use of his acoustic stimulation equipment and Shan Kuang for technical assistance.

LITERATURE CITED

Abercrombie M. 1946. Estimation of nuclear population from microtome sections. Anat Rec 94:239–247.

Bianchi LM, Gray NA. 2002. EphB receptors influence growth of ephrin-B1-positive statoacoustic nerve fibers. Eur J Neurosci 16:1499–1506.

Brors D, Bodmer D, Pak K, Aletsee C, Schafers M, Dazert S, Ryan AF. 2003. EphA4 provides repulsive signals to developing cochlear ganglion neurites mediated through ephrin-B2 and -B3. J Comp Neurol 462:90–100.

Brown MC, Liu TS. 1995. Fos-like immunoreactivity in central auditory neurons of the mouse. J Comp Neurol 357:85–97.

Cang J, Kaneko M, Yamada J, Woods G, Stryker MP, Feldheim DA. 2005. Ephrin-as guide the formation of functional maps in the visual cortex. Neuron 48:577–589.

Cant NB, Benson CG. 2003. Parallel auditory pathways: projection patterns of the different neuronal populations in the dorsal and ventral cochlear nuclei. Brain Res Bull 60:457–474.

Cowan CA, Henkemeyer M. 2002. Ephrins in reverse, park and drive. Trends Cell Biol 12:339–346.

Cowan CA, Yokoyama N, Bianchi LM, Henkemeyer M, Fritzsch B. 2000. EphB2 guides axons at the midline and is necessary for normal vestibular function. Neuron 26:417–430.

Cramer KS. 2005. Eph proteins and the assembly of auditory circuits. Hear Res 206:42–51.

Cramer KS, Rosenberger MH, Frost DM, Cochran SL, Pasquale EB, Rubel EW. 2000. Developmental regulation of EphA4 expression in the chick auditory brainstem. J Comp Neurol 426:270–278.

Cramer KS, Karam SD, Bothwell M, Cerretti DP, Pasquale EB, Rubel EW. 2002. Expression of EphB receptors and EphrinB ligands in the developing chick auditory brainstem. J Comp Neurol 452:51–64.

Cramer KS, Bermingham-McDonogh O, Krull CE, Rubel EW. 2004. EphA4 signaling promotes axon segregation in the developing auditory system. Dev Biol 269:26–35.

Cramer KS, Cerretti DP, Siddiqui SA. 2006. EphB2 regulates axonal growth at the midline in the developing auditory brainstem. Dev Biol 295:76–89.

Dalva MB, McClelland AC, Kayser MS. 2007. Cell adhesion molecules: signalling functions at the synapse. Nat Rev Neurosci 8:206–220.

Dravis C, Yokoyama N, Chumley MJ, Cowan CA, Silvany RE, Shay J, Baker LA, Henkemeyer M. 2004. Bidirectional signaling mediated by ephrin-B2 and EphB2 controls urorectal development. Dev Biol 271: 272–290.

Dufour A, Seibt J, Passante L, Depaepe V, Ciossek T, Frisen J, Kullander K, Flanagan JG, Polleux F, Vanderhaeghen P. 2003. Area specificity and topography of thalamocortical projections are controlled by ephrin/Eph genes. Neuron 39:453–465.

Ehret G, Fischer R. 1991. Neuronal activity and tonotopy in the auditory system visualized by *c-fos* gene expression. Brain Res 567:350–354.

Ellis J, Liu Q, Breitman M, Jenkins NA, Gilbert DJ, Copeland NG, Tempest HV, Warren S, Muir E, Schilling H, et al. 1995. Embryo brain kinase: a novel gene of the eph/elk receptor tyrosine kinase family. Mech Dev 52:319–341.

Feldheim DA, Kim YI, Bergemann AD, Frisen J, Barbacid M, Flanagan JG. 2000. Genetic analysis of ephrin-A2 and ephrin-A5 shows their requirement in multiple aspects of retinocollicular mapping. Neuron 25:563–574.

Feldheim DA, Nakamoto M, Osterfield M, Gale NW, DeChiara TM, Rohatgi R, Yancopoulos GD, Flanagan JG. 2004. Loss-of-function analysis of EphA receptors in retinotectal mapping. J Neurosci 24:2542–2550.

Flanagan JG, Vanderhaeghen P. 1998. The ephrins and Eph receptors in neural development. Annu Rev Neurosci 21:309–345.

Friauf E. 1992. Tonotopic order in the adult and developing auditory system of the rat as shown by c-fos immunocytochemistry. Eur J Neurosci 4:798–812.

Friauf E. 1995. C-fos immunocytochemical evidence for acoustic pathway mapping in rats. Behav Brain Res 66:217–224.

Friauf E, Lohmann C. 1999. Development of auditory brainstem circuitry. Activity-dependent and activity-independent processes. Cell Tissue Res 297:187–195.

Frisen J, Yates PA, McLaughlin T, Friedman GC, O'Leary DD, Barbacid M. 1998. Ephrin-A5 (AL-1/RAGS) is essential for proper retinal axon guidance and topographic mapping in the mammalian visual system. Neuron 20:235–243.

Gale NW, Holland SJ, Valenzuela DM, Flenniken A, Pan L, Ryan TE, Henkemeyer M, Strebhardt K, Hirai H, Wilkinson DG, Pawson T, Davis S, Yancopoulos GD. 1996. Eph receptors and ligands comprise two major specificity subclasses and are reciprocally compartmentalized during embryogenesis. Neuron 17:9–19.

Garel S, Rubenstein JL. 2004. Intermediate targets in formation of topographic projections: inputs from the thalamocortical system. Trends Neurosci 27:533–539.

Grunwald IC, Korte M, Adelmann G, Plueck A, Kullander K, Adams RH, Frotscher M, Bonhoeffer T, Klein R. 2004. Hippocampal plasticity requires postsynaptic ephrinBs. Nat Neurosci 7:33–40.

Hansen MJ, Dallal GE, Flanagan JG. 2004. Retinal axon response to ephrin-as shows a graded, concentration-dependent transition from growth promotion to inhibition. Neuron 42:717–730.

Henkemeyer M, Marengere LE, McGlade J, Olivier JP, Conlon RA, Holmyard DP, Letwin K, Pawson T. 1994. Immunolocalization of the Nuk receptor tyrosine kinase suggests roles in segmental patterning of the brain and axonogenesis. Oncogene 9:1001–1014.

Himanen JP, Chumley MJ, Lackmann M, Li C, Barton WA, Jeffrey PD, Vearing C, Geleick D, Feldheim DA, Boyd AW, Henkemeyer M, Nikolov DB. 2004. Repelling class discrimination: ephrin-A5 binds to and activates EphB2 receptor signaling. Nat Neurosci 7:501–509.

Hoffpauir BK, Grimes JL, Mathers PH, Spirou GA. 2006. Synaptogenesis of the calyx of Held: rapid onset of function and one-to-one morphological innervation. J Neurosci 26:5511–5523.

Holmberg J, Frisen J. 2002. Ephrins are not only unattractive. Trends Neurosci 25:239–243.

Hsieh CY, Hong CT, Cramer KS. 2007. Deletion of the Eph receptor EphA4 enhances deafferentation-induced ipsilateral sprouting in auditory brainstem projections. J Comp Neurol 504:508–518.

Huffman KJ, Cramer KS. 2007. EphA4 misexpression alters tonotopic projections in the auditory brainstem. Dev Neurobiol 67:1655–1668.

Kaur S, Lazar R, Metherate R. 2004. Intracortical pathways determine breadth of subthreshold frequency receptive fields in primary auditory cortex. J Neurophysiol 91:2551–2567.

Kil J, Kageyama GH, Semple MN, Kitzes LM. 1995. Development of ventral cochlear nucleus projections to the superior olivary complex in gerbil. J Comp Neurol 353:317–340.

Kim G, Kandler K. 2003. Elimination and strengthening of glycinergic/GABAergic connections during tonotopic map formation. Nat Neurosci 6:282–290.

Kovacs KJ. 1998. c-Fos as a transcription factor: a stressful (re)view from a functional map. Neurochem Int 33:287–297.

Leake PA, Snyder RL, Hradek GT. 2002. Postnatal refinement of auditory nerve projections to the cochlear nucleus in cats. J Comp Neurol 448: 6–27.

Leighton PA, Mitchell KJ, Goodrich LV, Lu X, Pinson K, Scherz P, Skarnes WC, Tessier-Lavigne M. 2001. Defining brain wiring patterns and mechanisms through gene trapping in mice. Nature 410:174–179.

Mann F, Harris WA, Holt CE. 2004. New views on retinal axon development: a navigation guide. Int J Dev Biol 48:957–964.

Marquardt T, Shirasaki R, Ghosh S, Andrews SE, Carter N, Hunter T, Pfaff SL. 2005. Coexpressed EphA receptors and ephrin-A ligands mediate opposing actions on growth cone navigation from distinct membrane domains. Cell 121:127–139.

McLaughlin T, O'Leary DD. 2005. Molecular gradients and development of retinotopic maps. Annu Rev Neurosci 28:327–355.

McLaughlin T, Hindges R, Yates PA, O'Leary DD. 2003. Bifunctional action of ephrin-B1 as a repellent and attractant to control bidirectional branch extension in dorsal-ventral retinotopic mapping. Development 130:2407–2418.

Mikaelian DO, Warfield D, Norris O. 1974. Genetic progressive hearing loss in the C57–b16 mouse. Relation of behavioral responses to chochlear anatomy. Acta Otolaryngol 77:327–334.

Morgan JI, Curran T. 1989. Calcium and proto-oncogene involvement in the immediate-early response in the nervous system. Ann N Y Acad Sci 568:283–290.

Murai KK, Nguyen LN, Irie F, Yamaguchi Y, Pasquale EB. 2003. Control of hippocampal dendritic spine morphology through ephrin-A3/EphA4 signaling. Nat Neurosci 6:153–160.

Ouagazzal AM, Reiss D, Romand R. 2006. Effects of age-related hearing loss on startle reflex and prepulse inhibition in mice on pure and mixed C57BL and 129 genetic background. Behav Brain Res 172:307–315.

Person AL, Cerretti DP, Pasquale EB, Rubel EW, Cramer KS. 2004. Tonotopic gradients of Eph family proteins in the chick nucleus laminaris during synaptogenesis. J Neurobiol 60:28–39.

Pfeiffenberger C, Yamada J, Feldheim DA. 2006. Ephrin-As and patterned retinal activity act together in the development of topographic maps in the primary visual system. J Neurosci 26:12873–12884.

Pickles JO, Claxton C, Van Heumen WR. 2002. Complementary and layered expression of Ephs and ephrins in developing mouse inner ear. J Comp Neurol 449:207–216.

Prakash N, Vanderhaeghen P, Cohen-Cory S, Frisen J, Flanagan JG, Frostig RD. 2000. Malformation of the functional organization of somatosensory cortex in adult ephrin-A5 knock-out mice revealed by in vivo functional imaging. J Neurosci 20:5841–5847.

Reber M, Burrola P, Lemke G. 2004. A relative signalling model for the formation of a topographic neural map. Nature 431:847–853.

Rodenas-Ruano A, Perez-Pinzon MA, Green EJ, Henkemeyer M, Liebl DJ. 2006. Distinct roles for ephrinB3 in the formation and function of hippocampal synapses. Dev Biol 292:34–45.

Rogers JH, Ciossek T, Ullrich A, West E, Hoare M, Muir EM. 1999. Distribution of the receptor EphA7 and its ligands in development of the mouse nervous system. Brain Res Mol Brain Res 74:225–230.

Rouiller EM, Wan XS, Moret V, Liang F. 1992. Mapping of c-fos expression elicited by pure tones stimulation in the auditory pathways of the rat, with emphasis on the cochlear nucleus. Neurosci Lett 144:19–24.

Rubel EW, Fritzsch B. 2002. Auditory system development: primary auditory neurons and their targets. Annu Rev Neurosci 25:51–101.

Saint Marie RL, Luo L, Ryan AF. 1999a. Effects of stimulus frequency and intensity on c-fos mRNA expression in the adult rat auditory brainstem. J Comp Neurol 404:258–270.

Saint Marie RL, Luo L, Ryan AF. 1999b. Spatial representation of frequency in the rat dorsal nucleus of the lateral lemniscus as revealed by acoustically induced c-fos mRNA expression. Hear Res 128:70–74.

Sanes DH, Constantine-Paton M. 1985. The sharpening of frequency tuning curves requires patterned activity during development in the mouse, Mus musculus. J Neurosci 5:1152–1166.

Sato K, Houtani T, Ueyama T, Ikeda M, Yamashita T, Kumazawa T, Sugimoto T. 1993. Identification of rat brainstem sites with neuronal Fos protein induced by acoustic stimulation with pure tones. Acta Otolaryngol Suppl 500:18–22.

Schweitzer L, Cant NB. 1984. Development of the cochlear innervation of the dorsal cochlear nucleus of the hamster. J Comp Neurol 225:228–243.

Siddiqui SA, Cramer KS. 2005. Differential expression of Eph receptors and ephrins in the cochlear ganglion and eighth cranial nerve of the chick embryo. J Comp Neurol 482:309–319.

Snyder RL, Leake PA. 1997. Topography of spiral ganglion projections to cochlear nucleus during postnatal development in cats. J Comp Neurol 384:293–311.

Song L, McGee JA, Walsh EJ. 2006. Consequences of combined maternal, fetal and persistent postnatal hypothyroidism on the development of auditory function in Tshrhyt mutant mice. Brain Res 1101:59–72.

Webber A, Raz Y. 2006. Axon guidance cues in auditory development. Anat Rec A Discov Mol Cell Evol Biol 288:390–396.

Wilkinson DG. 2001. Multiple roles of EPH receptors and ephrins in neural development. Nat Rev Neurosci 2:155–164.

Woolf NK, Ryan AF. 1985. Ontogeny of neural discharge patterns in the ventral cochlear nucleus of the mongolian gerbil. Brain Res 349:131–147.

Yang Y, Saint Marie RL, Oliver DL. 2005. Granule cells in the cochlear nucleus sensitive to sound activation detected by Fos protein expression. Neuroscience 136:865–882.

Yates PA, Roskies AL, McLaughlin T, O'Leary DD. 2001. Topographic-specific axon branching controlled by ephrin-As is the critical event in retinotectal map development. J Neurosci 21:8548–8563.

Zheng QY, Johnson KR, Erway LC. 1999. Assessment of hearing in 80 inbred strains of mice by ABR threshold analyses. Hear Res 130:94–107.